

CHAPTER 53

THE "SWAN" WAVE MODEL FOR SHALLOW WATER

N. Booij¹, L.H. Holthuijsen¹ and R.C. Ris¹

ABSTRACT

The numerical model SWAN (Simulating WAves Nearshore) for the computation of wave conditions in shallow water with ambient currents is briefly described. The model is based on a fully spectral representation of the action balance equation with all physical processes modelled explicitly. No a priori limitations are imposed on the spectral evolution. This makes the model a third-generation model. In Holthuijsen et al. (1993) and Ris et al. (1994) test cases for propagation, generation and dissipation have been shown without currents. Current effects have now been added and academic cases are shown here. The model is also applied in a fairly academic case of a shallow lake (Lake George, Australia) and in a complex, realistic case of an inter-tidal area with currents (Friesche Zeegat, the Netherlands). The results are compared with observations. A new development to formulate the model on a curvi-linear grid to accommodate linkage to hydro-dynamic circulation models is presented and a first test is shown.

INTRODUCTION

Over the last decade, the traditional wave ray models in coastal engineering to compute waves in nearshore conditions are being replaced by models that formulate the wave evolution in terms of a spectral energy balance on a regular grid (or the action balance in the presence of ambient currents). In third-generation versions of such models the wave spectrum is allowed to evolve free of any a priori limitations and all relevant physical processes are represented explicitly in a discrete spectral formulation. Such a wave model (the SWAN model), with the inclusion of ambient currents is described here. Conceptually it is an extension of deep water third-generation wave models but the physical processes and the numerical techniques involved are more complicated. The SWAN wave model has been conceived to be a computationally feasible third-generation spectral wave model for waves in shallow water (including the surf zone) with ambient currents in a consulting environment with return times of less than 30 min on a desk top computer.

¹ Delft University of Technology, Department of Civil Engineering, P.O. Box 5048, 2600 GA Delft, Netherlands.

THE SWAN WAVE MODEL

The SWAN wave model (Ris et al., 1994) is a fully discrete spectral model based on the action balance equation which implicitly takes into account the interaction between waves and currents through radiation stresses (e.g., Phillips, 1977):

$$\frac{\partial}{\partial t} N(\sigma, \theta) + \nabla_{x,y} \cdot [c_{x,y} N(\sigma, \theta)] + \frac{\partial}{\partial \sigma} [c_{\sigma} N(\sigma, \theta)] + \frac{\partial}{\partial \theta} [c_{\theta} N(\sigma, \theta)] = \frac{S(\sigma, \theta)}{\sigma}$$

The first term in the left-hand side is the rate of change of action density in time, the second term is the rectilinear propagation of action in geographical x -, y -space. The third term describes the shifting of the relative frequency due to currents and time-varying depths with propagation velocity c_{σ} in σ -space. The fourth term represents the propagation in θ -space (depth- and current-induced refraction) with propagation velocity c_{θ} . The term $S(\sigma, \theta)$ at the right hand side of the action balance equation is the source term representing the growth by wind, the wave-wave interactions and the decay by bottom friction, whitecapping and depth-induced wave breaking.

To reduce computer time, we remove time from the action balance equation (i.e., $\partial/\partial t = 0$). This is acceptable for most coastal conditions since the residence time of the waves is usually far less than the time scale of variations of the wave boundary conditions, the ambient current, wind or the tide. For cases in which the time scale of these variations becomes important, i.e., variable incoming waves at the boundary, or variable winds or currents, a quasi-stationary approach can be taken by repeating the computations for predefined time intervals.

The formulations for the generation, the dissipation and the quadruplet wave-wave interactions are taken from the WAM model (WAM Cycle 3, WAMDI group, 1988 and optionally WAM Cycle 4, Komen et al., 1994 as presently operational at the European Centre for Medium Range Weather Forecasting). For the present study the formulations from WAM Cycle 3 are used. These are supplemented with a spectral version of the dissipation model for depth-induced breaking of Battjes and Janssen (1978) (with the maximum wave height to depth ratio from Nelson, 1987) and a recently formulated discrete interaction approximation for the triad wave-wave interactions (Eldeberly and Battjes, 1995).

Fully implicit numerical schemes are used in the SWAN model for propagation in both geographic space and spectral space (an iterative, forward-marching, four-sweep technique, Ris et al., 1994). This scheme is unconditionally stable in contrast with the explicit schemes of conventional spectral wave models which are only conditionally stable and which require therefore very small time steps in shallow water (typically 10 s for 100 m resolution in water depth of 10 m where in the SWAN model the time increment may be as large as 15 min). The formulation is basically in terms of finite differences on a regular, rectangular grid. This is inconvenient in regions with highly variable scales such as tidal inlets, tidal flats and

estuaries. Nesting of grids with decreasing resolution is the conventional approach in such cases but it requires extra computations. A variable resolution grid would avoid such extra computations, in particular if the grid would conform to the topography of the region. It would also accommodate the linkage with hydrodynamic circulation models which are often formulated on such grids. Such a curvilinear approach is implemented in the SWAN model by considering in the numerical scheme of each spatial grid point, two separate, non-equidistant finite up-wind differences in each of two orthogonal directions. For the x -direction this is for grid point i, j (the grid points are ordered in x, y -space):

$$\frac{\partial C_x N}{\partial x} \approx \left[\frac{[c_x N]_{i,j} - [c_x N]_{i-1,j}}{\Delta \bar{x}_1} \right] + \left[\frac{[c_x N]_{i,j} - [c_x N]_{i,j-1}}{\Delta \bar{x}_2} \right]$$

where $\Delta \bar{x}_1 = \Delta x_1 - (\Delta y_1 / \Delta y_2) \Delta x_2$, $\Delta \bar{x}_2 = \Delta x_2 - (\Delta y_2 / \Delta y_1) \Delta x_1$. The increments are $\Delta x_1 = x_{i,j} - x_{i-1,j}$, $\Delta x_2 = x_{i,j} - x_{i,j-1}$, $\Delta y_1 = y_{i,j} - y_{i-1,j}$ and $\Delta y_2 = y_{i,j} - y_{i,j-1}$.

PROPAGATION TESTS

In Holthuijsen et al. (1993) the excellent agreement for academic cases is shown between computed wave propagation and analytical solutions and wave ray solutions of the linear wave theory without ambient currents. A similar good agreement with ambient currents added is shown here. For this, consider current-induced refraction in deep water, of monochromatic, long-crested waves with a (significant) wave height of 1 m and a (peak) frequency of 0.1 Hz. In the SWAN computation these waves are simulated with a Gaussian-shaped frequency spectrum with 0.01 Hz standard deviation and a $\cos^{500}(\theta)$ -directional distribution. Consider first these waves propagating from a uniform up-wave boundary over a distance of 4000 m in a following or opposing current of which the speed increases from 0 m/s to 2 m/s in the down-wave direction (current direction 0° or 180° direction relative to the mean wave direction). Only whitecapping is activated in the computations (although its effect is marginal). The computational results in terms of (significant) wave height for this current-induced shoaling test are shown in Fig. 1. The agreement for these cases with linear theory is excellent as the computational errors are less than 0.5% for the significant wave height and less than 0.1° for the mean wave direction (both differences hardly noticeable in Fig. 1). Consider next the same waves slanting across a 4000 m wide current field of which the current speed increases from 0 m/s to 2 m/s across the width and the current direction is constant and parallel to the straight current field boundaries. The wave direction is either $+30^\circ$ or -30° relative to the current direction. The results for the significant wave height and the wave direction are also shown in Fig. 1. The agreement for these cases with linear theory is as good as in the current-induced shoaling test.

The propagation with the curvilinear formulation is tested here by comparing the computational results on a rectangular grid with those on a curvilinear grid near

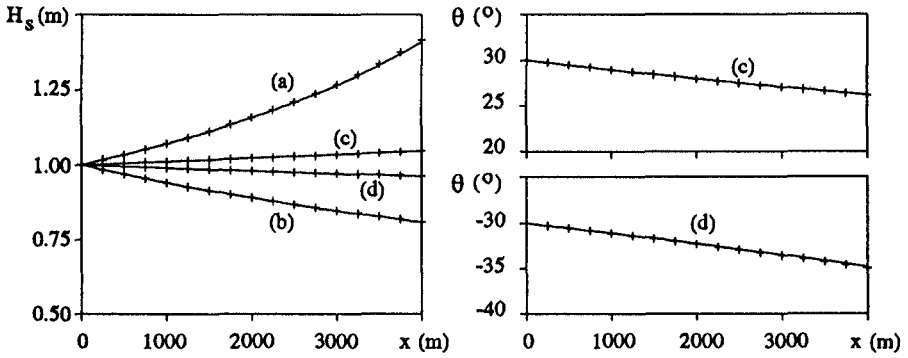


Fig. 1 Current-induced shoaling and refraction for monochromatic, long-crested waves for travelling against an opposing current (line a), a following current (line b) and a slanting current with incident wave direction $\theta_o=30^\circ$ (line c) and $\theta_o=-30^\circ$ (line d). Left panel: significant wave height H_s (m). Right panel: mean wave direction θ ($^\circ$), (—) analytical solutions and (+ + +) results from the SWAN model.

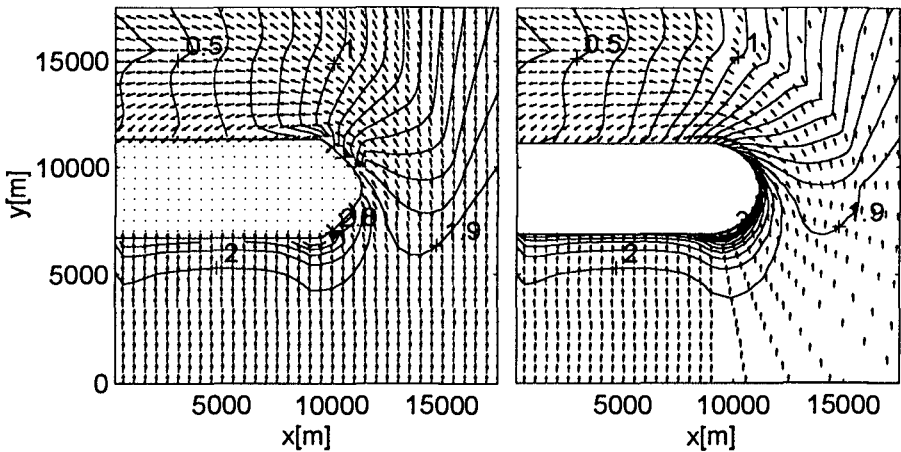


Fig. 2 The propagation of a short-crested wave field around a barrier island; significant wave height with contour line interval of 0.1 m and mean wave direction. The depth increases from the shore line over a distance of 4500 m to a constant water depth of 10 m. Left panel: computational results on a rectangular grid. Right panel: computational results on a curvi-linear grid (grid points at start of each vector).

a hypothetical barrier island (Fig. 2). All source terms are de-activated in these computations. The incoming waves are characterized with a JONSWAP spectrum with a $\cos^4(\theta)$ -directional distribution. The significant wave height and the mean wave period are 2.0 m and 6.0 s, respectively. The results of the computation on the curvi-linear grid agrees well with the results on the rectangular grid (Fig. 2).

WIND-WAVE GENERATION IN SHALLOW WATER

The observations of Young and Verhagen (1996) in the shallow Lake George (Australia) provide an excellent opportunity to test the generation of waves in the SWAN model in shallow water. These observations were carried out at eight wave stations in the lake, the bathymetry of which is fairly flat with an average depth of 2m (Fig. 3).

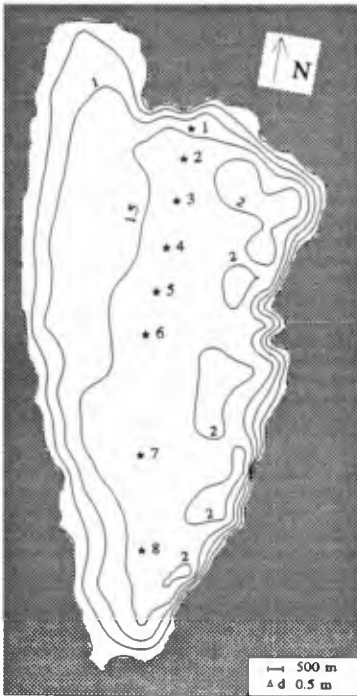


Fig. 3 Bathymetry of Lake George and the locations of the eight wave stations. Isolines represent depth contours (interval 0.5 m).

One case with a relatively high wind speed of $U_{10}=15.2$ m/s (at station 6 on 02-11-1992 at 16:00 local time) from northerly directions is chosen to demonstrate the performance of the SWAN model. From wind measurements at other stations it was found that the wind speed varied slightly along the north-south axis of the lake. This variation is calculated with the simple expression of Tayler and Lee (1984) proposed for these cases by Young and Verhagen (1996). As the up-wave coast line was not very well defined in this case (due to a very gentle bottom slope) the up-wind boundary condition was taken to be the observed wave spectrum at station 1. Fig. 4 shows the good agreement between the observed

significant wave height and peak frequency (I.R. Young and L.A. Verhagen, private communication, 1996) and the computational results. The inclusion of depth-induced wave breaking in modelling such conditions is unusual. Its effect is determined here by repeating the computation with this process de-activated in the model. The effect is significant only at the down-wind end of the lake (Fig. 4) and only for these high wind speeds (computations with wind speeds less than 10 m/s do not show this effect).

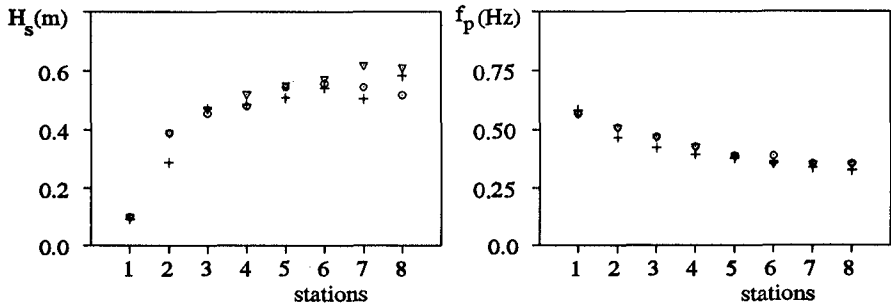


Fig. 4 Model results and observations of the significant wave height (left panel) and peak frequency (right panel) at the observation stations in Lake George for $U_{10}=15.2$ m/s. (+) measurements, (o) SWAN results, (v) SWAN results with depth-induced wave breaking de-activated.

APPLICATION

The performance of the SWAN model is shown here for a field case with wind and complex bottom and current patterns and 95% reduction in wave energy. It is a case in the Friesche Zeegat (the Netherlands) where a system of narrow channels (10 km length scale) runs from the North Sea into an area of tidal flats (the Wadden Sea, Fig. 5, the two main channels are about 10 m and 14 m deep). The waves were measured with one WAVEC pitch-and-roll buoy (station 1) at the deep water boundary of the area and five Waverider buoys (stations 2 to 6) located along the two channels (see Fig. 5). The observations that have been selected from the extensive data set for this verification are a flood current case which occurred on 09-10-1992 at 05:00 UTC (J.G. de Ronde and J.H. Andorka Gal, private communication, 1996). The reasons for this selection are that (a) at this time relatively high waves were observed (significant wave height about 2.5 m) which were generated by a storm in the northern North Sea, (b) during the period of observation the wind speed and direction were nearly constant, (c) the frequency spectrum was uni-modal and (d) tidal currents and water levels were measured. The wind velocity of $U_{10}=11.5$ m/s and direction of 320° are assumed to be uniform over the Friesche Zeegat area. The corresponding currents and water levels in the area were computed with a shallow water circulation model, resulting in a maximum current speed of about 1 m/s.

The spectrum at the up-wave boundary in deep water for the computations is taken equal to the frequency spectrum observed by the WAVEC buoy at station 1. It is taken uniform along a straight line through the location of the WAVEC buoy and roughly parallel with the 20 m depth contour. The observed significant wave height is $H_s = 2.24$ m and the mean wave period is $T_{m01} = 5.6$ s. The observed overall mean wave direction is 328° (nautical convention) and the overall directional width of the waves is 31° . The directional distribution is correspondingly

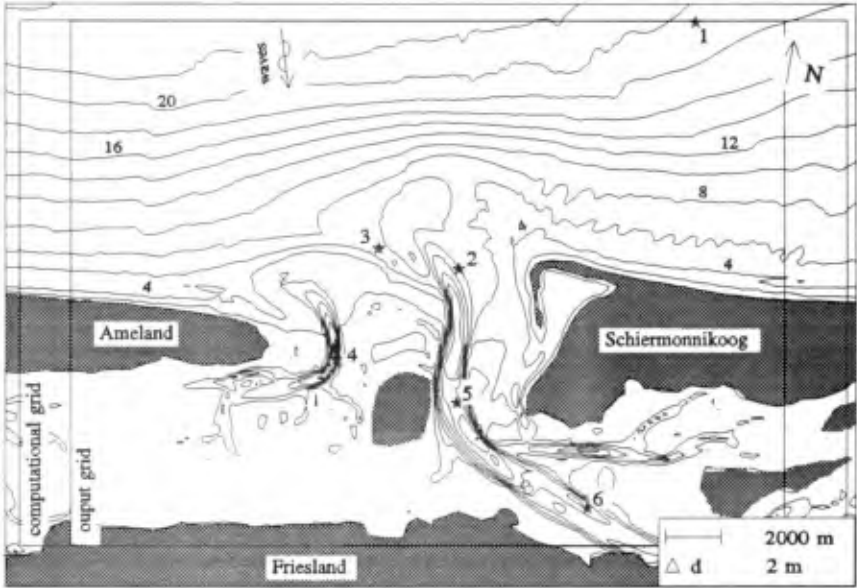


Fig. 5 The bathymetry of the Friesche Zeegat with the locations of the six stations. The isolines represent depth contours (interval 2 m). All water depths are in m.

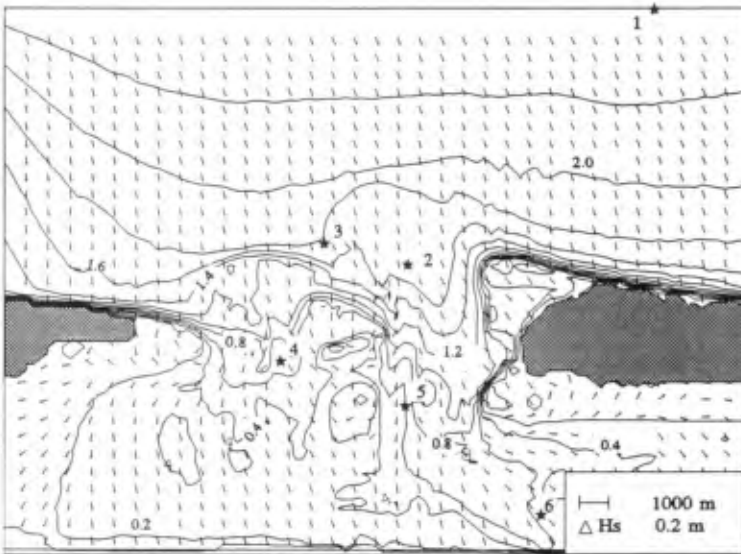


Fig. 6 Computed wave height pattern and mean wave direction (denoted with vectors) for a flood current case in the Friesche Zeegat. The isolines represent wave height contours (interval 0.2 m).

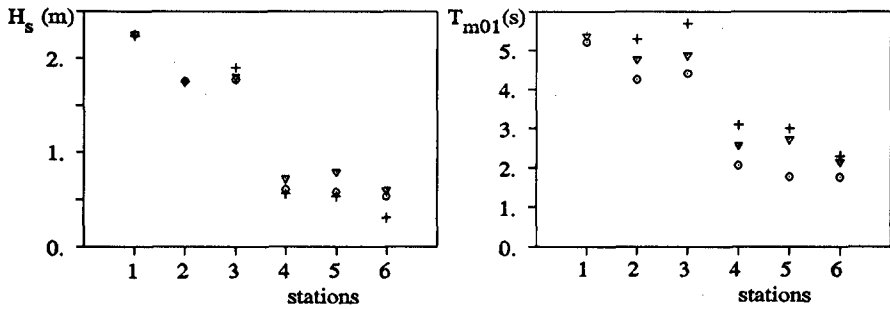


Fig. 7 Computed and observed significant wave height (left panel) and mean wave period (right panel) at the observation stations for the flood current case in the Friesche Zeegat: (+) observations, (o) SWAN results, (v) SWAN results without currents.

approximated with a $\cos^{2.1}(\theta)$ -directional distribution at all frequencies. The computed pattern of the significant wave height is shown in Fig. 6. This pattern is consistent with the pattern of the observations: the wave height gradually decreases between the deep water boundary and the entrance of the tidal inlet. Due to depth effects, more wave energy penetrates into the deeper eastern entrance than into the shallower western entrance of the tidal inlet (roughly 20 % lower wave height near station 4 than in the other entrance). As the waves penetrate through the tidal gap into the inlet they refract laterally to the shallower parts of the tidal inlet. They completely reverse direction behind the two barrier islands. The mean wave period (not shown here) follows roughly the same pattern. The effect of currents is shown with results of computations without currents (Fig. 7). This effect is evident but generally not very important in this case.

The calculated significant wave heights and mean wave periods at the six observation stations are given in Fig. 7. The agreement with the observations is fairly reasonable although the model tends to underestimate the mean wave period.

CONCLUSIONS

The SWAN wave model, which has been conceived as a computationally feasible third-generation spectral wave model for waves in shallow water (including the surf zone) with ambient currents for engineering consultancy has been implemented. It accounts for all relevant processes of propagation, generation, dissipation and nonlinear wave-wave interactions (except diffraction but including depth-induced wave breaking, triad wave-wave interactions and the effects of currents). Tests so far in academic conditions and in realistic field conditions show good agreement between computational results and observations although the present version of the model tends to slightly underestimate the mean wave period.

The present computation time is 6×10^{-5} s per grid point in x -, y -, σ -, θ -space per iteration on a HP 9000/735 work station (without currents; three times more than this when currents are included). A typical engineering application (without currents) of 100×100 geographic (water covered) grid points, 24 frequencies and 36 directions with 3 to 5 iterations will therefore take typically between 30 and 45 min computation time. With the expected performance of desk-top computers presently entering the market this will reduce to less than 15 - 30 min within the next few years. The operational goal has therefore been achieved. Future versions of the SWAN model (presently under development) will be non-stationary, formulated on a curvi-linear grid, and optionally formulated in spherical coordinates with a higher-accuracy propagation scheme and possibly include the effects of diffraction and reflections.

ACKNOWLEDGEMENTS

We gratefully acknowledge the generosity of I.R. Young and L.A. Verhagen of the University of New South Wales in Australia and of J.G. de Ronde, J.H. Andorka Gal and their colleagues from the Ministry of Transport and Public Works in the Netherlands in sharing their data from Lake George and the Friesche Zeegat, respectively. We are equally grateful to B.A.J. Les from the Delft University of Technology who (at the Ministry of Transport and Public Works) carried out the calculations for the currents and water levels in the Friesche Zeegat.

REFERENCES

- Battjes, J.A. and J.P.F.M. Janssen, 1978, Energy loss and set-up due to breaking of random waves, 16th Int. Conf. Coastal Engineering, ASCE: 569 - 587
- Eldeberky, Y. and J.A. Battjes, 1995, Parameterization of triad interactions in wave energy models, Coastal Dynamics '95, W.R. Dally and R.B. Zeidler (Eds.), ASCE: 140-148
- Holthuijsen, L.H., N. Booij and R.C. Ris, 1993, A spectral wave model for the coastal zone, 2nd International Symposium on Ocean Wave Measurement and Analysis, New Orleans, Louisiana, July 25-28, 1993, New York, pp. 630-641
- Komen, G.J., L. Cavaleri, M. Donelan, K. Hasselmann, S. Hasselmann and P.A.E.M. Janssen, 1994, Dynamics and Modelling of Ocean Waves, Cambr. Univ. Press, 532 p.
- Nelson, R.C., 1987, Design wave heights on very mild slopes, Civil Eng. Trans., Inst. Eng. Aust., 29, 157-161
- Ris, R.C., L.H. Holthuijsen and N. Booij, 1994, A spectral model for waves in the near shore zone, 24th Int. Conf. Coastal Engng, Kobe, Oct. 1994, pp. 68-78
- WAMDI group: S. Hasselmann, K. Hasselmann, E. Bauer, P.A.E.M. Janssen, G.J. Komen, L. Bertotti, P. Lionello, A. Guillaume, V.C. Cardone, J.A. Greenwood, M. Reistad, L. Zambresky and J.A. Ewing, 1988, The WAM model - a third generation ocean wave prediction model, J. Phys. Oceanogr., Vol. 18: 1775-1810
- Young, I.R. and L.A. Verhagen, 1996: The growth of fetch limited waves in water of finite depth. Part I: Total Energy and peak frequency, Coastal Engineering, Vol. 29, pp. 47-78
- Taylor, P.A. and R.J. Lee, 1984: Simple guidelines for estimating wind speed variations due to small-scale topographic features, Climatol. Bull., 18, 3-32